iJRASET
International Journal For Research in Applied Science and Engineering Technology

INTERNATIONAL JOURNAL FOR RESEARCH

IN APPLIED SCIENCE & ENGINEERING TECHNOLOGY

Volume: 5 **Issue:** VII **Month of publication:** July 2017

DOI:

www.ijraset.com

Call: 08813907089 | E-mail ID: ijraset@gmail.com

International Journal for Research in Applied Science & Engineering Technology (IJRASET)
ISSN: 2321-9653; IC Value: 45.98; SJ Impact Factor:6.887
Volume 5 Issue VII, July 2017- Available at www.ijraset.com

Robust Adaptive Nonlinear Yaw Tracker Design for Unmanned Hover Vehicle

Sannan Sajid Khan[1], Muhammad Talha Munir[2], Zarak Avais Khan[3], Rabbaya Akhtar[4]
[1,2,3,4]*Department of Electrical Engineering, COMSATS Institute of Information Technology Wah Cantt 47040, Punjab, Pakistan*

Abstract*: *An Unmanned Hover Vehicle is a hovering platform over a cushion of air with many practical applications and it also acts as a testbed for simulation and verification of control algorithms. The control of yaw or steering dynamics of a double propeller Unmanned Hover Vehicle using robust adaptive nonlinear control method has been considered. The system parameters are assumed unknown and the technique of nonlinear adaptation using manifold immersion is performed for their estimation. Reference tracking is obtained. The complete system simulation is performed and controller is tuned using rapid prototyping. The theoretically proposed controller is validated experimentally. The discrete time realization of control algorithm is implemented on digital controller, which is interfaced in real time with Simulink. The potential of proposed algorithm relies upon the flexibility in the structure of control algorithm and promising transient behaviour of the closed loop system dynamics.
Keywords:* *Unmanned Hover Vehicle, Double Rotor, Adaptive Control, Robust Control, Rapid Control Prototyping.

I. INTRODUCTION

An Unmanned Hover Vehicle (UHV) is an airborne vehicle that lies in the domain of Remotely Operated Vehicles (ROV) that hover over the air cushion. It has various commercial applications as well as military uses. It has no crew so it presents many advantages in military applications and dangerous or tedious environmental conditions by reducing risk of loss of human life and time saving. They can be deployed to perform tasks such as mine counter measures, surveillance and reconnaissance, anti-airborne warfare, fast attack craft, combat training, oil and gas exploration and construction, aerial data collection, disaster monitoring and environmental surveys.

There is a boom in the development of UHVs over past few decades. The unpredictable environmental conditions and complex dynamics of UHVs make them a challenging system to be modelled and controlled. It also acts as a benchmark to simulate and test new and advanced control techniques. A mini UHV typically has nonlinear dynamics. Moreover, by involving dynamics of the driving motor-propeller actuator along with the motor amplifier, complicates the problem still more as it adds more state variables in system dynamics, which tantamount to increase in the order of the system. To add to the difficulty, there are various uncertain system parameters. Hence there is always a room for a better and effective control technique for UHVs.

There are various control techniques available in literature. Sliding mode tracking control of surface vessels is considered in [1]. A study on control technology of double rotor permanent magnet synchronous motor actuated vehicle is presented in details in [2]. Fuzzy heading control of a rotary electric propulsion ship with double propellers is presented with experimental results in [3]. Hybrid rotational and revolving simulation of propeller in aircraft with two propellers by fractal animation model is included in [4], which is based on shifting centroid method in double mode from a fixed point. A control system for double rotor unmanned hover vehicle is presented in [5]. Modelling, manoeuvring analysis and course following for two unmanned surface vehicles driven by a single propeller and double propellers is investigated in [6], which also includes theoretical simulation and experimental results. A controller design for a multi-fan hovering system is presented in [7]. Sliding mode control of ship electric propulsion system is investigated in [8].

Most of these techniques consider the linear system model or a reduced order model of the system. Moreover, controllers do not have many tuneable parameters to gain much control over system responses. Many controllers suffer degradation of response as the operation conditions change or the system parameters vary with time. We have applied a robust adaptive nonlinear control algorithm that relies on robustification of reduced order system controller against full order system dynamics [9]. The controller is also robust against unknow system parameters and has a lot of free tuneable parameters to gain control over feedback dynamic response of the system output. mail.

II. HARDWARE OVERVIEW

A hover vehicle has a suction pump that forces the air out of the bottom tube, hence creating an air cushion, which lifts the vehicle above ground. Once in hover mode, two thrusters take over the motion of the vehicle. It is shown in Fig. 1. The actual experimental

ISSN: 2321-9653; IC Value: 45.98; SJ Impact Factor:6.887
Volume 5 Issue VII, July 2017- Available at www.ijraset.com

setup used in this work is shown in Fig. 2. It is used for experimental verification of control algorithm. This setup incorporates digital controller, sensors, actuators, aircraft body and transceivers, as will be described in the detail shortly. This hardware setup provides a means for the implementation of hardware in loop Rapid Control Prototyping scheme, for real time data monitoring and control

Fig. 1 A practical hover vehicle(left) and its functional description (right)

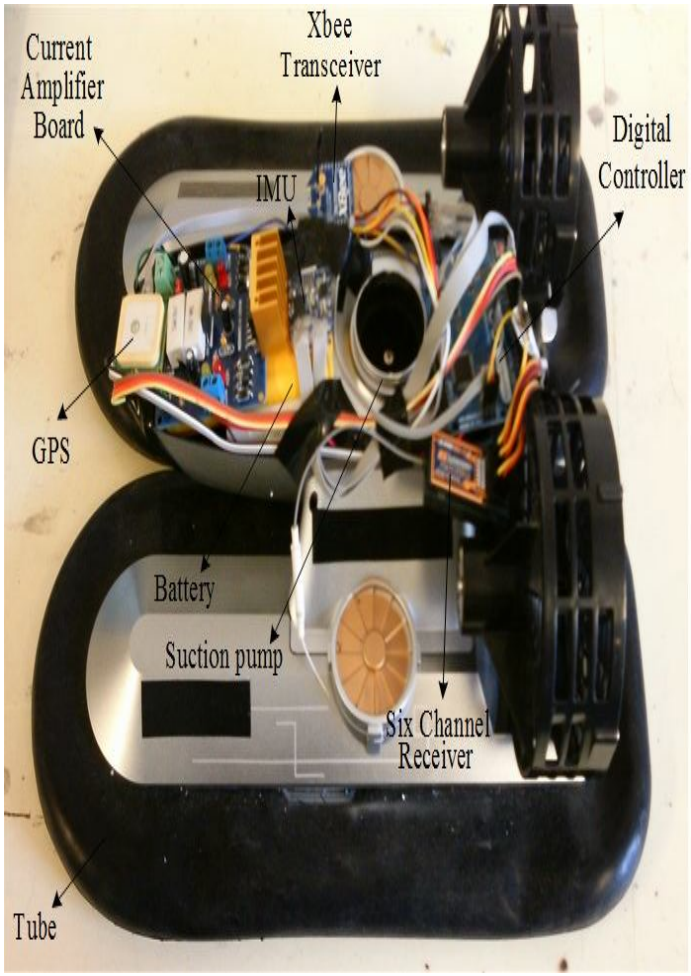

Fig. 2 Overview of the hardware system

ISSN: 2321-9653; IC Value: 45.98; SJ Impact Factor:6.887
Volume 5 Issue VII, July 2017- Available at www.ijraset.com

Fig. 3 shows the schematic diagram for the front view of the hardware setup. It consists of two thrust producing motors. Their thrust forces are labelled F_1 and F_2. These forces produce two counter torques around the center of mass of the aircraft body and producing a resultant yaw maneuver θ, as well as lift on the aircraft body. The objective is to control the amplitudes of these two forces such as to track a yaw reference with inadequate knowledge of system parameters.

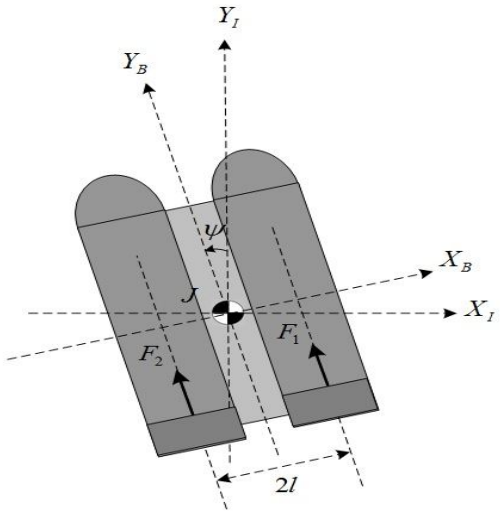

Fig. 3 A practical hover vehicle(left) and its functional description (right)

III.THE CONTROL ALGORITHM SYNTHESIS

Consider a nonlinear parameter uncertain system,

$$\dot{\underline{p}} = \underline{s}\left(\underline{p}, u_e\right) = \underline{f}\left(\underline{p}\right) + \underline{g}\left(\underline{p}\right)u_e \qquad (1)$$

where $\underline{p} \in \mathbb{R}^n$ and $u_e \in \mathbb{R}^m$. The state vector $\underline{p}$ evolves on a smooth manifold P of dimension n, which is spanned by tangential manifold to the system map $\underline{s}$. The system map $\underline{s}$ in (1) has been decomposed into a drift vector field $\underline{f}(.)$ and a controlled vector field $\underline{g}$. In (1), $u_e \in U\left(\underline{p}\right)$ is the system forcing function with U a state dependent input set which belongs to the control bundle $\bigcup_{\underline{p}\in \mathrm{P}} U\left(\underline{p}\right)$. The topological manifold immersion based nonlinear control approach involves defining a reduced order exosystem. The state trajectories of the exosystem evolve on a C^∞ submanifold $\mathrm{Q} \subset \mathrm{P}$. The problem of controller design then boiled down to synthesize a control law that dynamically immerses the state trajectories of full order system to the manifold Q. Let us consider an exosystem with state vector $\underline{q} \in \mathbb{R}^q$ with $q < n$, which contains origin in its reachable set. This can be achieved by defining the vector field $\underline{\Upsilon}\left(\underline{q}\right)$ of the exosystem that governs the evolution of $\underline{q}$ as given by (2).

$$\dot{\underline{q}} = \underline{\Upsilon}\left(\underline{q}\right) \qquad (2)$$

Defining a smooth submanifold for the exosystem of (2) as:

$$\mathrm{Q} = \left\{\underline{p} \in \mathbb{R}^n \middle| \underline{p} = \underline{\psi}\left(\underline{q}\right); \underline{q} \in \mathbb{R}^q\right\} \qquad (3)$$

The controlled integral curves of system map $\underline{s}$ can be attracted by the submanifold Q if partial differential (4) along with the condition in (5) is satisfied [9].

$$\underline{f}\left(\underline{\psi}\left(\underline{q}\right)\right) + \underline{g}\left(\underline{\psi}\left(\underline{q}\right)\right)\wp\left(\underline{\psi}\right) = L_{\Upsilon}\underline{\psi} \qquad (4)$$

$$\underline{q}(t) = \underline{0} \quad \forall \quad \underline{q}(0) \in \mathbb{R}^2 \text{ as } \mathrm{t} \to \infty \qquad (5)$$

Here $L_{\underline{\Upsilon}}\underline{\psi} = (\nabla_{\underline{q}}\underline{\psi})\underline{\Upsilon}(\underline{q})$ is the so-called Lie derivative. Also $\wp(\underline{\psi}(\underline{q})) = v(\underline{\psi}(\underline{q}),0)$ on the submanifold Q and $u = v(\underline{p},\zeta(\underline{p}))$ is the synthesized feedback control law that renders Q attractive. $\zeta(.)$ is the implicit description of Q and it is given by parameterized form in (6).

$$\zeta(\underline{p}) = \underline{p} - \underline{\psi}(\underline{q}) = 0 \tag{6}$$

Introducing state variable $\hbar$ to define "off" the submanifold Q dynamics given by:

$$\dot{\hbar} = L_{\underline{s}}\zeta\big|_{u=\vartheta(\underline{p},\hbar)} = \left(\frac{\partial\zeta}{\partial\underline{q}}\right)\underline{s}(\underline{p},\vartheta(\underline{p},\hbar)) \tag{7}$$

In terms of $\hbar$ and any constant $\alpha > 0$, the synthesized controller ϑ the system mapping is given by,

$$\dot{\underline{p}} = \underline{s}(\underline{p},\vartheta(\underline{p},\hbar)) \tag{8}$$

For any general system of form,

$$\begin{aligned}\dot{\underline{p}}_1 &= \underline{\xi}_1(p_1) + \underline{\xi}_2(\underline{p}_1)p_2\\ \dot{p}_2 &= \underline{\varphi}(\underline{p})^T\underline{\lambda}_1 + \lambda_2 u\end{aligned} \tag{9}$$

where $\underline{\xi}_i(.)$ and $\underline{\varphi}(.)$ are smooth mappings, λ_i are unknown parameters and $\dot{\underline{p}}_1 = \underline{\xi}_1(\underline{p}_1)$ is globally stable, then for constants $\varepsilon > 0$ and $k > 0$, the geometric adaptive estimates of λ_i are given by [9].

$$\dot{\hat{\underline{\lambda}}} = -\left(I + \nabla_{\underline{\lambda}}\underline{\upsilon}\right)^{-1}\left(\left(\nabla_{\underline{p}}\underline{\upsilon}\right)\left(\underline{\xi}_1(\underline{p}_1) + \underline{\xi}_2(\underline{p}_1)p_2\right) + \frac{\partial\underline{\upsilon}}{\partial p_2}\left(-kp_2 - \varepsilon L_{\underline{\xi}_1}V_1(\underline{p}_1)\right)\right) \tag{10}$$

and the corresponding geomantic synthesized control law is given by,

$$u = -\left(\hat{\lambda}_2 + \upsilon_2(\underline{p},\hat{\underline{\lambda}}_1)\right)\left(kp_2 + \varepsilon L_{\underline{\xi}_2}V_1(\underline{p}_1) + \varphi(\underline{p})^{\mathrm{T}}\left(\hat{\underline{\lambda}}_1 + \underline{\upsilon}_1(\underline{p})\right)\right) \tag{11}$$

The vector $\underline{\upsilon} = \left[\underline{\upsilon}_1(\underline{p}) \quad \upsilon_2(\underline{p},\hat{\underline{\lambda}}_1)\right]^{\mathrm{T}}$ is given by:

$$\underline{\upsilon}_1(\underline{p}) = \gamma_1\int_0^{p_2}\varphi(\underline{p}_1,\eta)d\eta \tag{12}$$

$$\upsilon_2(\underline{p},\hat{\underline{\lambda}}_1) = \gamma_2\left(k\frac{p_2}{2} + \varepsilon L_{\underline{\xi}_2}V_1(\underline{p}_1)p_2\right) + \gamma_2\int_0^{p_2}\varphi(\underline{p}_1,\eta)^{\mathrm{T}}\left(\hat{\underline{\lambda}}_1 + \underline{\upsilon}_1(\underline{p}_1,\eta)\right)d\eta \tag{13}$$

Here $V_1(\underline{p}_1)$ is any mapping such that for some class-K function $\kappa(.)$, we have,

$$L_{\underline{\xi}_1}V_1(\underline{p}_1) \le -\kappa(\underline{p}_1) \tag{14}$$

and $\gamma_1 > 0$, $\gamma_2 > 0$ are constants [9].

IV. SYSTEM DYNAMICS AND CONTROL

Consider the experimental testbed of twin rotor mechanism in the Fig. 2. If ψ denotes yaw angle of main rod and ω denotes the angular speed of main rotor motor then the system state variables for yaw dynamics are described by (15).

$$\underline{p} = \left[p_1 \quad p_2 \quad p_3\right]^{\mathrm{T}} = \left[\psi \quad \dot{\psi} \quad \omega\right]^{\mathrm{T}} \tag{15}$$

If we consider the second order curve fit for the static thrust calibration of main rotor against its driving signal using arrangement in Fig. 3, and results in Fig. 4, then the dynamics of system are described by following system of (16). Force decomposition is shown in Fig. 5.

$$\begin{aligned}\underline{f}(\underline{p}) &= \left[p_2 \quad -k_1p_2 + k_2p_3^{\,2} \quad -p_3k_3\right]^{\mathrm{T}}\\ \underline{g}(\underline{p}) &= \left[0 \quad 0 \quad k_4\right]^{\mathrm{T}}\\ \underline{s}(\underline{p},u_e) &= \left[p_3 \quad -k_1p_2 + k_2p_3^{\,2} \quad -p_3k_3 + k_4u_e\right]^{\mathrm{T}}\end{aligned} \tag{16}$$

Now (2) and (8) evaluate to following expressions.

$$\underline{\Upsilon}(\underline{q}) = \begin{bmatrix} q_2 & -k_1 + k_2\varsigma_1^{\,2} \end{bmatrix}^{\mathrm{T}} \tag{17}$$

$$\underline{p} = \underline{\psi}(\underline{q}) = \begin{bmatrix} q_1 & q_2 & \psi_1(q_1, q_2) \end{bmatrix}^{\mathrm{T}} \tag{18}$$

$$\vartheta(\underline{p}, \hbar) = \frac{-\alpha\hbar + \dot{\varsigma}_1 + k_3 p_3}{k_4} \tag{19}$$

The reduced order system is given by (20).

$$\begin{aligned} \dot{\hbar} &= -\alpha\hbar \\ \dot{p}_1 &= p_2 \\ \dot{p}_2 &= -k_1 p_2 + k_2\varsigma_1^{\,2} \\ \dot{p}_3 &= -\alpha\hbar + \dot{\varsigma}_1 \end{aligned} \tag{20}$$

The system in (20) immerses to system described by (21).

$$\begin{aligned} \dot{p}_1 &= p_2 \\ \dot{p}_2 &= -k_1 + k_2\varsigma_1^{\,2} \end{aligned} \tag{21}$$

Let us consider feedback linearization of (21) as,

$$\varsigma_1 = \sqrt{u} : u > 0 \tag{22}$$

The immersion control law is given by,

$$\vartheta(\underline{p}, \hbar) = \frac{-\alpha\hbar + \dot{\varsigma}_1 + k_3 p_3}{k_4} \tag{23}$$

Using (21) and (22) we get,

$$\underline{\dot{p}} = \begin{bmatrix} p_2 & -k_1 p_2 + k_2 u \end{bmatrix}^{\mathrm{T}} \tag{24}$$

For the estimation of unknown parameters in (24), using the results in (9) through (14), we get.

$$\underline{\xi}_1(p_1) = 0, \quad \underline{\xi}_2(\underline{p}_1) = 1, \quad \lambda_1 = k_1, \quad \lambda_2 = k_2 > 0, \quad \varphi(\underline{p}) = -1 \tag{25}$$

$$L_{\underline{\xi}_2} V_1(\underline{p}_1) = 2\underline{p}_1 \tag{26}$$

$$\underline{\upsilon} = \begin{bmatrix} c_1 p_2 \\ c_2 p_2^2 +_1 c_3 \hat{\lambda}_1 p_2 + c_4 p_1 p_2 \end{bmatrix} \tag{27}$$

$$\nabla_{\underline{\hat{\lambda}}} \underline{\upsilon} = \begin{bmatrix} 0 & 0 \\ -\gamma_2 p_2 & 0 \end{bmatrix} \tag{28}$$

$$\nabla_{\underline{p}_1} \underline{\upsilon} = \frac{\partial \underline{\upsilon}}{\partial p_1} = \begin{bmatrix} 0 & 2\varepsilon\gamma_2 p_2 \end{bmatrix}^{\mathrm{T}} \tag{29}$$

$$\frac{\partial \underline{\upsilon}}{\partial p_2} = \begin{bmatrix} -\gamma_1 & k\gamma_2 p_2 + 2\gamma_2 k p_1 - \gamma_2\hat{\lambda}_1 + \gamma_1\gamma_2 p_2 \end{bmatrix}^{\mathrm{T}} \tag{30}$$

The parameter estimates in (10) leads us to,

$$\underline{\dot{\hat{\lambda}}} = \begin{bmatrix} c_5 p_1 + c_6 p_2 \\ c_7 p_1^2 + c_8 p_2^2 + c_9 p_1 p_2 + c_{10} p_2\hat{\lambda}_1 + c_{11} p_1\hat{\lambda}_1 \end{bmatrix} \tag{31}$$

The control law in terms of estimates parameters is given by,

$$u = -\left(\hat{\lambda}_2 + \upsilon_2(\underline{p}, \hat{\underline{\lambda}}_1)\right)\left(kp_2 + 2\varepsilon p_1 - \hat{\underline{\lambda}}_1 - \underline{\upsilon}_1(\underline{p})\right) \quad (32)$$

At the last the reference tracking is achieved by modifications of control law as,

$$\vartheta'(\underline{p}, \hbar) = \frac{-\alpha\hbar + \dot{\varsigma}_1 + k_3 p_3}{k_4} + \sigma(t) \quad (33)$$

A typical classical proportional derivative tracker law can be used to follow reference command as given by,

$$\sigma(t) = \Xi(e(t)) \quad (34)$$

$$\Xi(.) = -\frac{k_3}{k_4}\left(k_p(.) + k_d\frac{d(.)}{dt}\right) \quad (35)$$

The control law in (33) can be split to produce drive signals of two motors according to the splitter algorithm given by (36).

$$\vartheta_1 = \begin{cases} \left|\vartheta' - \vartheta'_m\right| + \vartheta_{1_{th}} & if \quad (\vartheta' - \vartheta'_m) > 0 \\ \vartheta_{1_{th}} & if \quad (\vartheta' - \vartheta'_m) < 0 \end{cases}, \quad \vartheta_2 = \begin{cases} \left|\vartheta' - \vartheta'_m\right| + \vartheta_{2_{th}} & if \quad (\vartheta' - \vartheta'_m) < 0 \\ \vartheta_{2_{th}} & if \quad (\vartheta' - \vartheta'_m) > 0 \end{cases} \quad (36)$$

$\vartheta_{i_{th}}$ is the upper threshold value of i^{th} motor drive signal dead zone and ϑ'_m is the mean value of signal ϑ'.

V. SIMULATION AND TESTING

The values of various system parameters are given in Table 1.

TABLE I
VALUES OF SYSTEM PARAMETERS

Parameter	Value	Parameter	Value
k_3	145	c_4	0.018
k_4	7.15	c_5	-0.25
k	61	c_6	-214
γ_1	4.1	c_7	5×10^{-4}
γ_2	1.0	c_8	845.0
ε	2.1×10^{-3}	c_9	0.25
c_1	-6.25	c_{10}	-750.0
c_2	72.0	c_{11}	-0.05
c_3	-3.25	c_{12}	0.125

Using above values the closed loop system is simulated in Fig. 4.

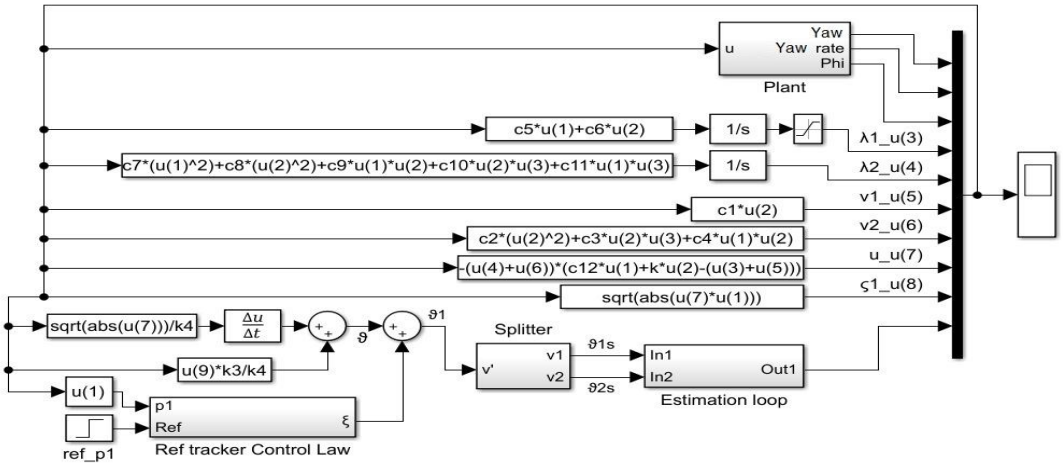

Fig. 4 Simulation of system in MATLAB/Simulink

ISSN: 2321-9653; IC Value: 45.98; SJ Impact Factor:6.887
Volume 5 Issue VII, July 2017- Available at www.ijraset.com

The simulation result for yaw reference tracking response is shown in Fig. 5. The response is stable with zero steady state error. The simulation result for the yaw rate response is shown in Fig. 6. The yaw rate decays to zero within 1.5 seconds. The simulation result for manipulated variables response is shown in Fig. 6. The magnitude of variables is within practical limits and drives the plant output to the desired reference signal.

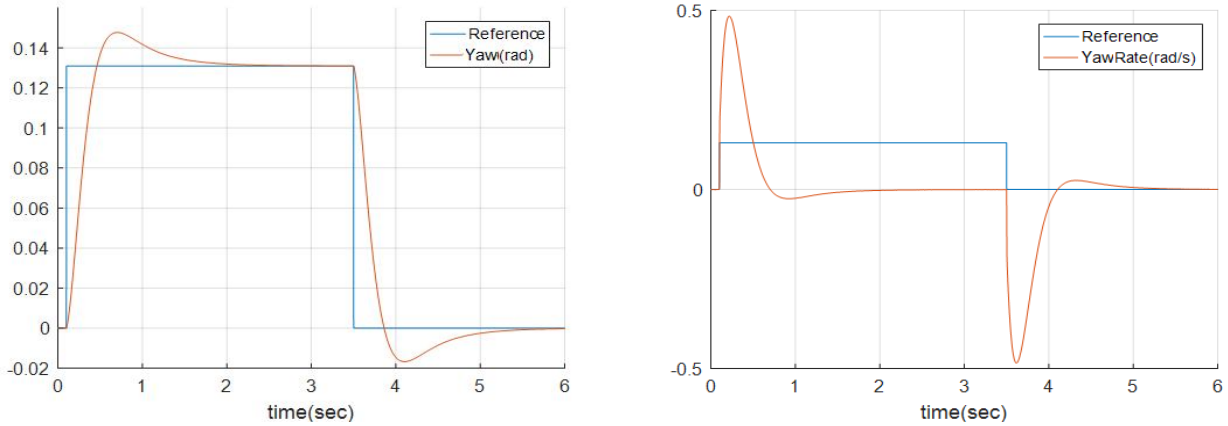

Fig. 5 Yaw reference tracking(left); Yaw rate response(right)

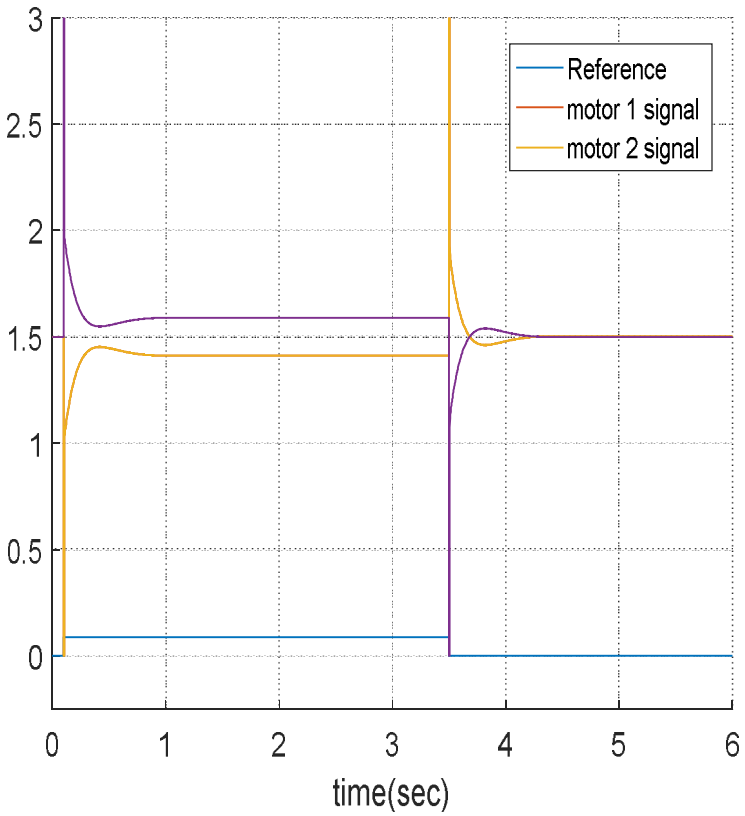

Fig. 6 Manipulated variables during reference tracking

The experimental RCP Simulink model of the closed loop system with reference tracker is shown in Fig. 7. The schematic representation of experimental hardware setup is shown in Fig. 8. The completes experimental setup is shown in Fig. 9, which shows the components of ground station as well as the UHV.

ISSN: 2321-9653; IC Value: 45.98; SJ Impact Factor:6.887
Volume 5 Issue VII, July 2017- Available at www.ijraset.com

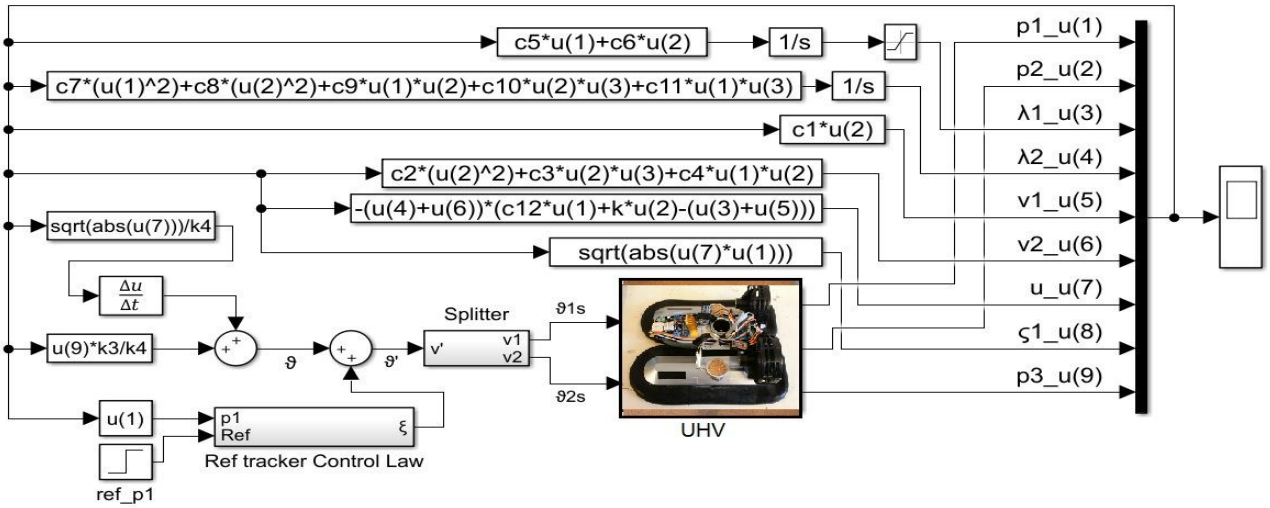

Fig. 7 Hardware operation in RCP mode for controller tunning.

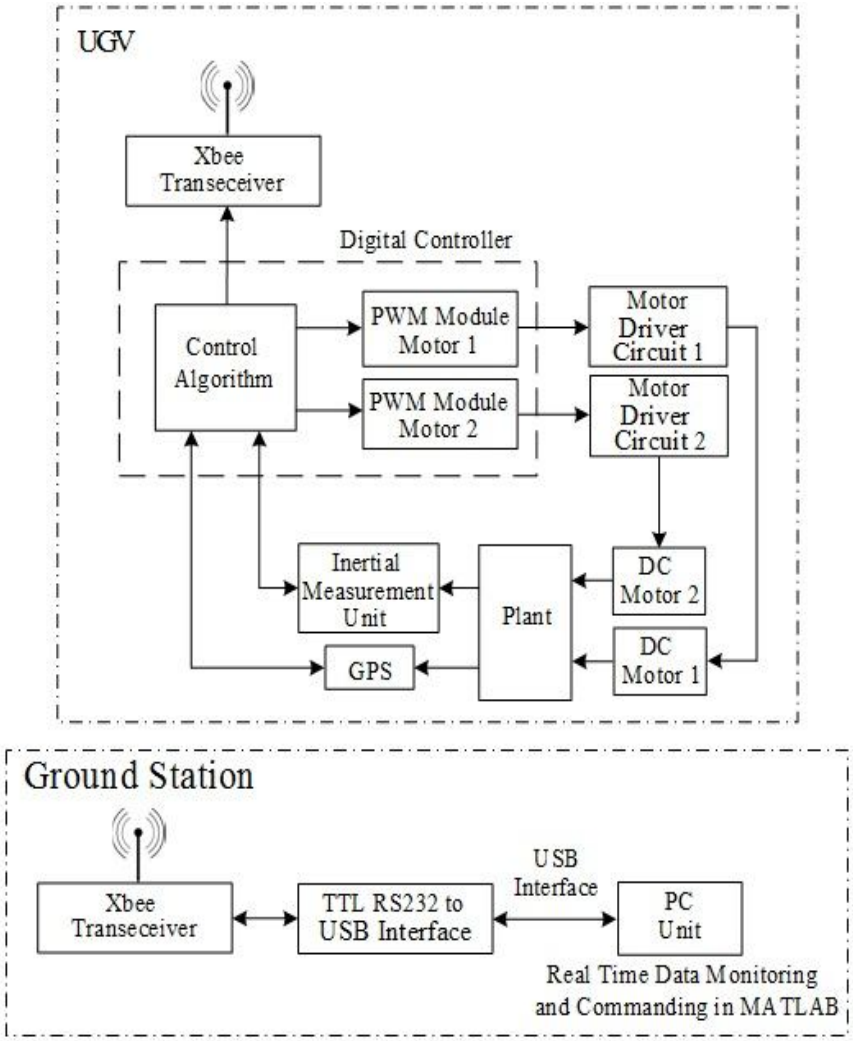

Fig. 8 Schematic representation of the whole system

ISSN: 2321-9653; IC Value: 45.98; SJ Impact Factor:6.887
Volume 5 Issue VII, July 2017- Available at www.ijraset.com

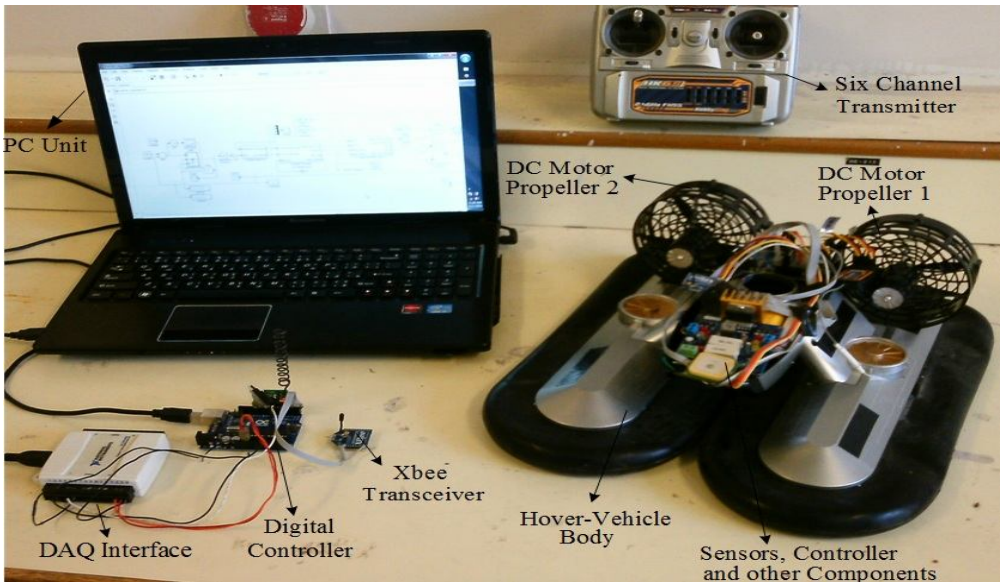

Fig. 9 The complete experimental setup

The experimental result for yaw reference tracking response is shown in Fig. 10. The response is stable with zero steady state error. The simulation result for the yaw rate response is shown in Fig. 10. The yaw rate decays to zero within 1.5 seconds. The simulation result for manipulated variables response is shown in Fig. 11. The magnitude of variables is within practical limits and drives the plant output to the desired reference signal.

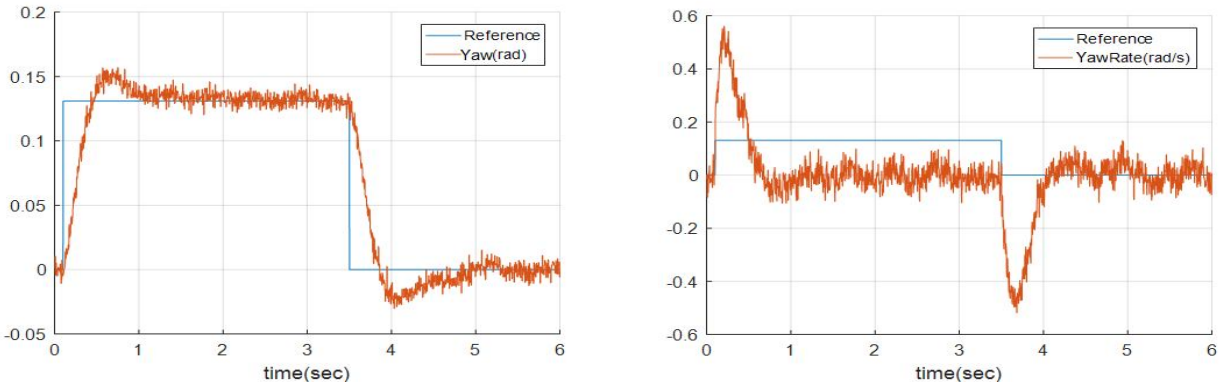

Fig. 10 Yaw reference tracking(left); Yaw rate response(right)

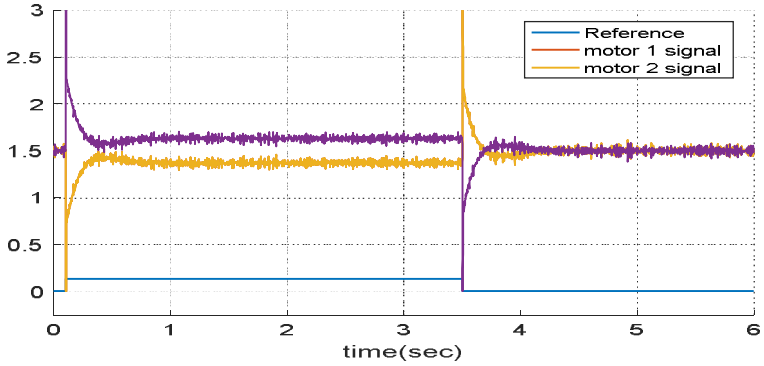

Fig. 11 Manipulated variables during reference tracking

ISSN: 2321-9653; IC Value: 45.98; SJ Impact Factor:6.887
Volume 5 Issue VII, July 2017- Available at www.ijraset.com

VI. CONCLUSIONS

A robust nonlinear adaptive controller for the yaw dynamics of a double rotor unmanned hover vehicle has been presented. System parameters are considered unknown and they are estimated using nonlinear adaptation. The proposed control technique is simulating in Simulink. The theoretical technique is tested in real time using digital controllers interfaced in real time with Simulink. The control algorithm has a lot of free tunable parameters. The results showed promising behavior of closed loop system in the presence of parameters uncertainties. Moreover, a greater control of closed loop system dynamics is possible owing to the flexibility in control algorithm.

REFERENCES

[1] H. Ashrafiuon and K. R. Muske, "Sliding mode tracking control of surface vessels," 2008 American Control Conference, Seattle, WA, 2008, pp. 556-561.
[2] F. Zhang, Z. Meng and J. Chen, "Study on control technology of double rotor PMSM in underwater vehicle," 2009 International Conference on Applied Superconductivity and Electromagnetic Devices, Chengdu, 2009, pp. 295-298.
[3] S. Sun, N. Wang, Y. Liu and B. Dai, "Fuzzy heading control of a rotary electric propulsion ship with double propellers," Proceedings of the 33rd Chinese Control Conference, Nanjing, 2014, pp. 4598-4602.
[4] T. Darmanto, I. S. Suwardi and R. Munir, "Hybrid rotational and revolving simulation of propeller in aircraft with two propellers by fractal animation model: Based on shifting centroid method in double mode from a fixed point," 2014 International Conference on Computer, Control, Informatics and Its Applications (IC3INA), Bandung, 2014, pp. 166-171.
[5] Q. Zhu, "Design of control system of USV based on double propellers," 2013 IEEE International Conference of IEEE Region 10 (TENCON 2013), Xi'an, 2013, pp. 1-4.
[6] J. Jiu-cai, Z. Jie and S. Feng, "Modelling, manoeuvring analysis and course following for two unmanned surface vehicles driven by a single propeller and double propellers," The 27th Chinese Control and Decision Conference (2015 CCDC), Qingdao, 2015, pp. 4932-4937.
[7] B. Luce and K. Rahnamai, "Controller design for a multi-fan hovering system," Proceedings: Electrical Insulation Conference and Electrical Manufacturing and Coil Winding Conference (Cat. No.01CH37264), Cincinnati, OH, 2001, pp. 311-317.
[8] H. Dallagi and S. Nejim, "Sliding mode control of ship electric propulsion system," 2015 IEEE 12th International Multi-Conference on Systems, Signals & Devices (SSD15), Mahdia, 2015, pp. 1-7.
[9] A. Astolfi and R. Ortega, “Immersion and Invariance: a new tool for stabilization and adaptive control of nonlinear systems”, IEEE Trans. on Automatic Control, 48(4), 2003, pp. 590–606.

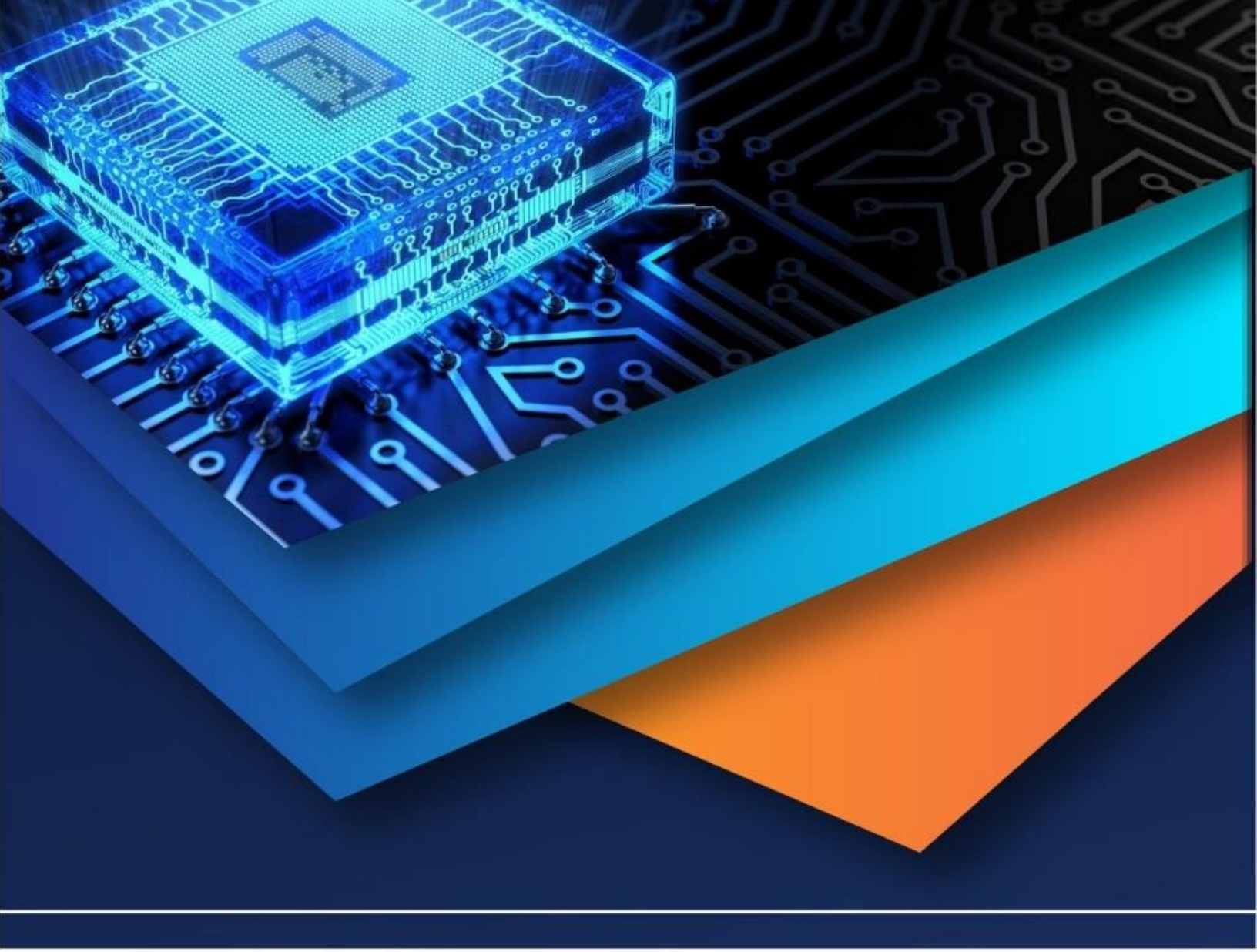

10.22214/IJRASET

45.98

IMPACT FACTOR: 7.129

IMPACT FACTOR: 7.429

INTERNATIONAL JOURNAL FOR RESEARCH

IN APPLIED SCIENCE & ENGINEERING TECHNOLOGY